End-on and Side-on Nematic Liquid Crystal Dendrimers

Laura Pastor,[†] Joaquín Barberá,[†] Mark McKenna,[†] Mercedes Marcos,*[,†] Rafael Martín-Rapún,[†] José Luis Serrano,[†] Geoffrey R. Luckhurst,[‡] and Azizah Mainal[‡]

Química Orgánica, Facultad de Ciencias-Instituto de Ciencia de Materiales de Aragón,Universidad de Zaragoza-CSIC, 50009 Zaragoza, Spain, and School of Chemistry, University of Southampton, Highfield, Southampton SO17 1BJ, U.K.

Received July 28, 2004; Revised Manuscript Received September 9, 2004

ABSTRACT: A group of nematic materials based on poly(propyleneimine) dendrimers (PPI) containing two types of mesogenic subunits were synthesized. The presence of different types of mesogenic group, the topology of the attachment to the core (end-on and side-on), and the chemical nature of the linking connection to the PPI scaffold (imine or amide) were used to tailor the mesomorphic properties. The materials were characterized by a variety of techniques including ^{1}H, ^{13}C NMR spectroscopy, GPC, MALDI−TOF MS, DSC, POM, and X-ray diffraction. The crystalline state, when it exists, was found to be suppressed for most of the materials once they had undergone the first transition to the isotropic phase. The majority of the compounds exhibited glass transitions near to or lower than room temperature and an accompanying wide temperature range mesophase. All of the side-on dendrimers synthesized exhibit a nematic mesophase whereas end-on dendrimers exhibit different mesophases depending on the length of the terminal chain of the mesogenic unit (nematic for $n = 2, 4, 5$). The ^{2}H NMR technique was used to investigate the symmetry of the nematic phase formed by the side-on dendrimers ($G = 3$). These studies revealed that the symmetry of the nematic phase is uniaxial. They also allow the investigation of the orientational order of the phase and the rate of field-induced director alignment.

A new class of dendrimers which exhibit uniaxial nematic phases has been synthesized. These results indicate that the synthesis of these nanophase-structured dendrimers leads to macromolecules with LC properties similar to those of comparable low molar mass compounds.

Introduction

Dendritic materials have recently become of great interest in supramolecular chemistry, mainly due to the possibility of obtaining well-defined macromolecules.[1,2] One of our areas of interest concerns the way in which the structure of the peripheral units modifies the liquid crystalline properties of the dendrimer.[3] In this context, we have previously reported the synthesis and characterization of poly(amidoamine) PAMAM and poly(propyleneimine) PPI dendrimers in which the mesomorphism can be tuned to give lamellar or columnar arrangements depending on the structure of the peripherally attached promesogenic units.[3] The viscosity of these lamellar dendrimers is usually high, which would make the applicability of these materials very limited. One way to overcome this problem would be the use of less viscous mesomorphic dendrimers, which could be obtained if they displayed nematic mesophases.[4−10] With this aim in mind we envisaged two strategies to obtain nematic liquid crystal dendrimers. On one hand, we changed the terminal alkoxy chain ($OC_{10}H_{21}$)[11] of the promesogenic unit for a shorter one (OC_2H_5, OC_4H_9, OC_5H_{11}). On the other hand, we used an approach similar to that employed in side groups liquid crystalline polymers.[12,13] In these systems, it has been shown that the introduction of laterally attached mesogenic units makes it difficult for the units to adopt the side-by-side molecular arrangement typical of lamellar phases, thus favoring a nematic order.[3] In this paper we present the synthesis and the properties of side-on and end-on nematic liquid crystal dendrimers whose structures are shown in Scheme 1.

* To whom correspondence should be addressed. Fax: (+) 34 976 761209. Telephone: (+) 34.976 762076. E-mail: mmarcos@unizar.es.
[†] Universidad de Zaragoza.
[‡] University of Southampton.

Results and Discussion

General Synthetic Pathways. The synthesis of dendrimer series 1, which contain an end-on mesogen attached to the PPI ($G = 1, 2, 3, 4, 5$) is shown in Scheme 2.

The synthesis of end-on dendrimers was carried out in two steps following the method previously described.[11] First, synthesis of 4-(4-alkoxybenzoyloxy)-2-hydroxybenzaldehydes (**3**) were carried out in dichloromethane by reaction of 4-alkoxybenzoic acid (**1**) with 2,4-dihydroxybenzaldehyde (**2**) using *N,N′*-dicyclohexylcarbodiimide (DCC) as an esterification agent and 4-(dimethylamino)pyridine (DMAP) as a catalyst, according to the method described by Hassner and Alexanian.[14] Second, the dendrimers were obtained by condensation of 4-(4′-alkoxybenzoyloxy)-2-hydroxybenzaldehydes (**3**) with the terminal amino groups of the corresponding generation of PPI (**4**) using neutral alumina as a dehydrating agent. The final products were purified by column chromatography when the terminal chain was long, and by dissolving the product in dichloromethane, precipitating it with methanol and centrifuging several times until the dendrimers were free from lower molecular weight compounds.

The synthesis of series 2 which contain side-on mesogens attached to the PPI core ($G = 1, 2, 3, 4, 5$), is shown in Scheme 3.

The synthesis of the side-on promesogenic unit was carried out following a method described by Keller et

10.1021/ma048450p CCC: $27.50
Published on Web 11/11/2004

Scheme 1. Structures of the Dendrimers under Study

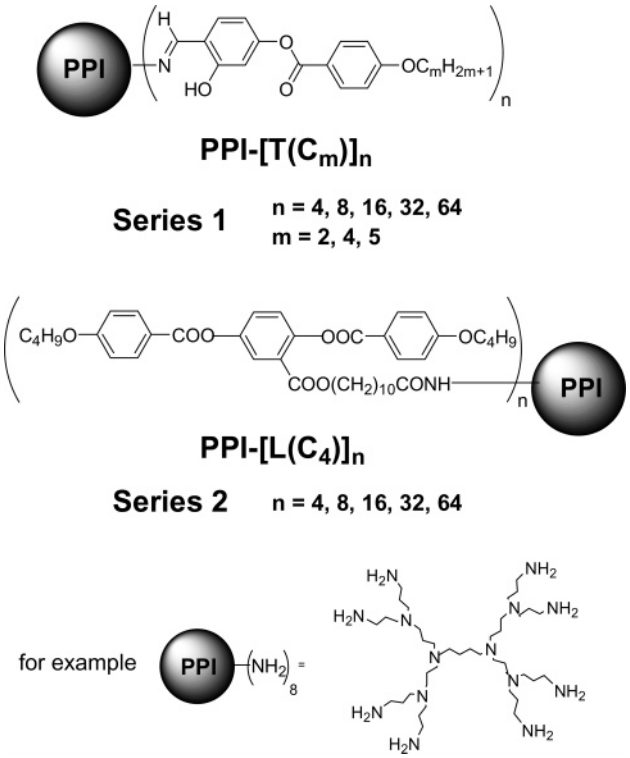

Scheme 2. Synthetic Route for the End-on Attached Mesogenic Dendrimers

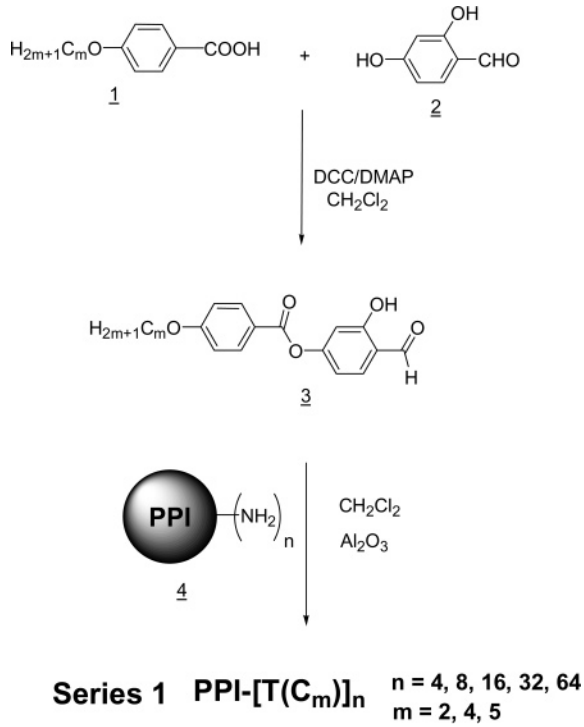

al..[15] Compound **10** was synthesized in the reaction between the sodium salt of 2,5-dihydroxybenzoic acid (**9**) and the bromo derivative **8** in DMF. The esterification of **10** with 4-butoxybenzoic acid (**11**), using DCC and DMAP, gave **12**, which was then deprotected with palladium hydroxide on carbon, and cyclohexene to yield **13**. Compound **15** was obtained by esterification of **13** with 2,3,4,5,6-pentafluorophenol (**14**). Finally, the pentafluorophenol ester **15** was coupled to different generations of poly(propyleneimine) (PPI) to give dendrimers

Scheme 3. Synthetic Route for the Side-on Attached Mesogenic Dendrimers

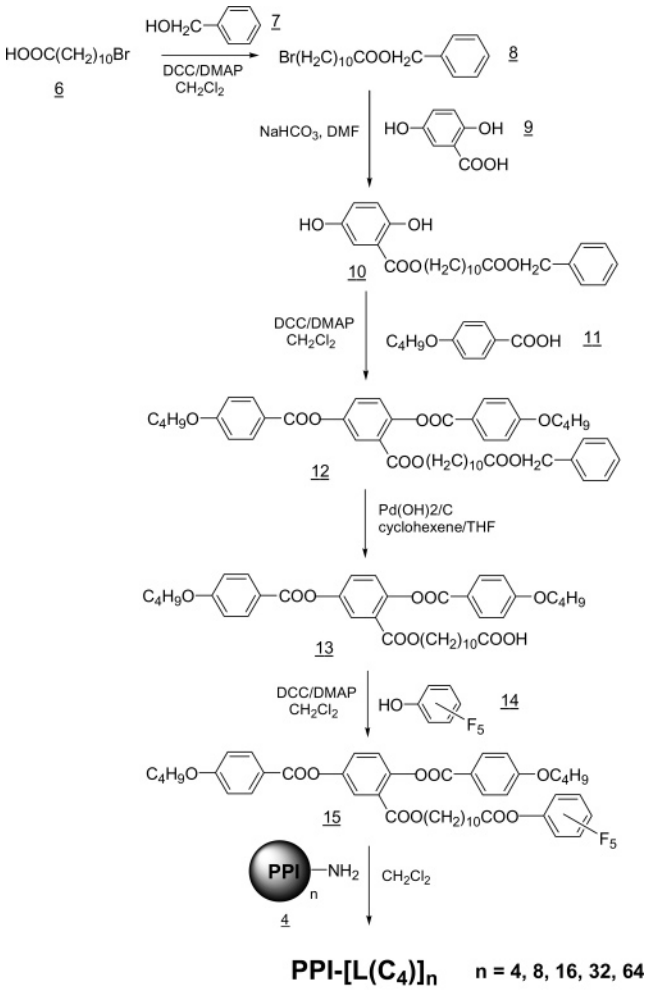

PPI-$[L(C_4)]_n$ (n = 4, 8, 16, 32, 64) where n equals the number of functional groups, by following a method similar to that described by Meijer.[16] This coupling was performed by the reaction of the amine-functionalized dendrimer with a small excess of pentafluoro derivative.

All of the compounds were isolated as air-stable yellow solids that are soluble in solvents such as dichloromethane, chloroform, and THF; they are insoluble in ethanol.

The dendrimers were characterized by ^{1}H NMR, ^{13}C NMR, IR spectroscopy, FAB$^+$, MALDI−TOF MS, gel permeation chromatography (GPC), and elemental analysis. All these techniques gave satisfactory results. ^{1}H NMR, ^{13}C NMR, and IR spectroscopy have proved to be very useful in confirming the structure and the purity of these materials.

In series 1, evidence for condensation reactions was provided by the lack of a signal at δ = 195 ppm in the ^{13}C NMR spectra (which corresponds to the carbonyl group of the aldehyde) along with the total absence of the NH_2 signals from the starting compound in the ^{1}H NMR and IR spectra.

In series 2, the complete amide bond formation was confirmed up to the technique sensitivity by the lack in ^{1}H NMR, and ^{13}C NMR spectra of signals at δ = 2.62 and δ = 41 ppm, respectively, corresponding to the methylene unit α to the primary amine groups of the starting dendrimers.

Table 1. MALDI−TOF and Elemental Analysis Data for the End-on Dendrimers (Series 1)

					% C, % H, % N	
	n	$M_{w(theor)}$	MALDI	$M_{w(exp)}/M_{w(theor)}$	calcd	found
OC_2H_5	4	1389.6	1389.5	1.00	69.1, 6.4, 6.0	68.9, 6.4, 6.0
	8	2919.3	2920.2	1.00	69.1, 6.6, 6.7	69.0, 6.7, 6.7
	16	5979.0	6000.3	1.00	69.1, 6.7, 7.0	67.2, 6.6, 6.9
	32	12098.3	10183	0.84	69.1, 6.8, 7.2	67.6, 6.9, 7.1
	64	24336.8	21738	0.89	69.1, 6.8, 7.3	68.8, 6.9, 7.4
OC_4H_9	4	1501.8	1501.7	1.00	70.4, 7.0, 5.6	70.2, 7.1, 5.6
	8	3143.8	3144.7	0.99	70.3, 7.2, 6.2	69.9, 7.3, 6.3
	16	6427.9	6429.0	1.00	70.3, 7.3, 6.5	69.7, 7.3, 6.5
	32	12996.0	11471.0	0.88	70.2, 7.3, 6.7	69.2, 7.3, 6.3
	64	26132.2	n.a.	n.a.	70.2, 7.3, 6.7	69.3, 7.4, 6.8
OC_5H_{11}	4	1557.9	1557.8	1.00	72.9, 7.2, 5.4	72.8, 7.2, 5.3
	8	3256.0	3256.7	1.00	70.8, 7.4, 6.0	71.1, 7.4, 6.2
	16	6652.3	6673.8	1.00	70.8, 7.5, 6.3	69.8, 7.5, 6.3
	32	13444.8	11428.1	0.85	70.8, 7.6, 6.5	69.7, 7.6, 6.6
	64	27029.9	n.a.	n.a.	70.7, 7.6, 6.5	69.8, 7.7, 6.6

[a] n.a.: not available.

Table 2. GPC and MALDI−TOF and Elemental Analysis Data for the Side-on Dendrimers (Series 2)

						% C, % H, % N	
n	$M_{w(theor)}$	MALDI	$M_{w(exp)}/M_{w(theor)}$	GPC	I_p	calcd	found
4	3009.7	3008.6	0.99	4499	1.01	71.0, 6.8, 2.8	70.8, 6.8, 3.0
8	6151.4	6156.7	1.00	16272	1.05	71.0, 6.9, 3.2	71.1, 7.0, 3.2
16	12443.0	12474.2	1.00	11241	1.09	70.7, 7.0, 3.4	70.7, 7.1, 3.5
32	25026.2	25031.0	1.00	15717	1.05	71.0, 7.0, 3.5	70.7, 7.0, 3.4
64	49611.8	45185.0	0.91	19687	1.04	72.4, 5.1, 3.6	72.3, 5.1, 3.6

In addition, the excellent solubility of these dendrimers in $CDCl_3$ allowed us to integrate the different peaks in the ^1H NMR spectra, confirming in all cases that the expected polymer has been obtained. These results are in agreement with the negative ones given by these materials in the ninhydrine test for primary amine groups.

To determine the molecular weight of these materials, accurately, MALDI−TOF MS experiments were carried out. Molecular ion data and elemental analysis data for the dendrimers synthesized are collected in Tables 1 and 2 for series 1 and 2, respectively.

GPC (mobile phase, CH_2Cl_2; calibration standard, polystyrene) confirmed the presence of practically monodisperse polymers in all cases. However, as is often the case with dendrimers, a marked deviation from the calculated molecular weight was found in the experimental data, even for the lower molecular weight compounds,[17] indicating a smaller "apparent" hydrodynamic volume, which is most probably due to the globular shape of the molecule in contrast with that of the coiled PS standards used.

Mesomorphic Properties. The mesomorphic properties of the materials were investigated by differential scanning calorimetry (DSC), polarizing optical microscope (POM), and X-ray diffraction. The phase transition temperatures, the associated enthalpy values and the normalized entropy ($\Delta S/R$) at the nematic-to-isotropic transition (when this is observed in the DSC) of the materials are given in Tables 3 and 4 for series 1 and 2, respectively.

Series 1. As can be seen in Table 1 all of the dendrimers synthesized for series 1 exhibit nematic liquid crystalline behavior. The mesophase textures were observed with a polarizing microscope using thin films of a sample mounted between a glass slide and a cover. The nematic mesophase was easily identified by the optical textures (see Figure 1). On cooling from the isotropic phase to the mesophase, they exhibit typical nematic droplets with the schlieren texture, which are similar to the descriptions of nematic textures given by Demus and Richter.[18]

Table 3. Transition Temperatures as Determined by DSC[a] in the Second Scan of the End-on Dendrimers (PPI-[T(C_m)]$_n$ (Series 1))

OC_mH_{2m+1}	n	transitions (°C) {ΔH (kJ mol^{-1})}
OC_2H_5	4	Ng 20 N 122[b] I
	8	Ng 19 N 110[b] I
	16	Ng 25 N 95[b] I
	32	Ng 16 N 8[b] I
	64	Cr 40 {181.07} N 100 {8.27} I
OC_4H_9	4	Ng 13 N 116 {3.30} I
	8	Ng 13 N 94 {0.31} I
	16	Ng 13 N 87 {5.21} I
	32	Ng 21 N 87 {9.10} I
	64	Ng 21 N 106 {39.20} I
OC_5H_{11}	4	Ng 11 N 70 {46.86} C 121 {103.24} I I 85 {2.10} N
	8	Ng 13 N 79 {2.12} I
	16	Ng 15 N 73 {4.52} I
	32	Ng 5 N 73[b] I
	64	Ng 18 N 101 {30.54} I

[a] Ng = nematic glass, Cr = crystal, N = nematic phase, I = isotropic liquid. [b] Optical data.

The DSC curves reveal a melting point and a clearing point for the first heating scan only in a few cases, most of the dendrimers synthesized exhibit a glass transition and an isotropization transition. However, in the second scan after an annealing process, very simple thermograms were obtained and only the glass transition and the isotropization transition could be observed for most of the dendrimers. The identity of the nematic mesophase was confirmed by X-ray measurements.

Series 2. As can be seen from Table 4, all of the side-on dendrimers of series 2 also exhibit nematic liquid crystalline behavior as the only mesophase, which was identified in each case by the schlieren texture observed by POM[18] with similar clearing points for all generations except $G = 5$ which is lower. In the DSC curves, we observe a broad crystal to isotropic liquid transition in the first heating cycle and only the glass transition

Table 4. Transition Temperatures As Determined by DSC[a] in the Second Scan of the Intermediates and the Side-on Dendrimers (PPI-[L(C$_4$)]$_n$ (Series 2))

n	transitions (°C) {ΔH (kJ mol^{-1})}	ΔH_{I-N}/m.u.[b] (kJ mol^{-1})	$(\Delta S_{mol}/R)n^{-1}$ [c]
-COOBn	Ng 0 N 58 {1.50} I		0.55
−COOH	Ng 9 N 49 {29.74} C 114 {74.89} I I 98 {3.50} N		1.14
−COOC$_6$F$_5$	N 32 {5.67} C$_1$ 55 {4.65} C$_2$ 73 {12.05} I I 75 {1.21} N		0.42
4	Ng 28 N 80 {4.09} I	1.02	0.35
8	Ng 30 N 78 {9.41} I	1.18	0.40
16	Ng 24 N 72 {13.69} I	0.86	0.32
32	Ng 31 N 78 {37.54} I	1.17	0.40
64	Ng 14 N 53 {59.53} I	0.93	0.35

[a] Ng = nematic glass, N = nematic, and I = isotropic liquid. [b] Enthalpy of the nematic-to-isotropic liquid transition per mesogenic unit. [c] Normalized transition entropy (n = number of mesogens).

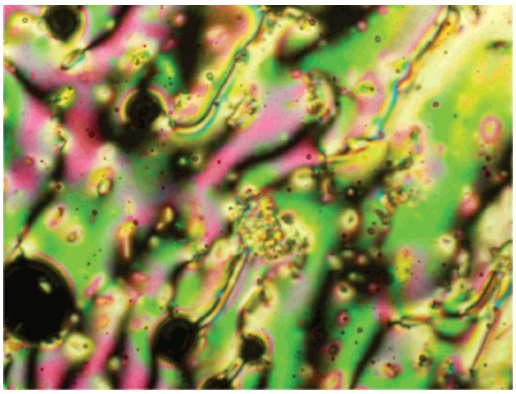

Figure 1. Optical texture of PPI-[T(C$_5$)]$_{16}$ observed in nematic mesophase under the polarizing microscope at 82 °C.

and the isotropization transition for the other cycles.

The enthalpy change at the nematic-to-isotropic liquid transition per mesogenic unit is about the same order of magnitude (0.86−1.28 kJ mol^{-1}) for all of the compounds; therefore, the strength of the interactions between mesogenic units are similar regardless of the number of units present in the molecule or the size of the PPI core. This suggests that the behavior of these compounds is mainly driven by the mesogenic units and is independent of the generation number.

X-ray Measurements. Four representative dendrimers were studied by X-ray diffraction (XRD) at room temperature in their glassy state (compounds in series 1 with $m = 2$, $n = 64$ (PPI-[T(C$_2$)]$_{64}$), with $m = 4$, $n = 16$ and 64 (PPI-[T(C$_4$)]$_{16}$ and PPI-[T(C$_4$)]$_{64}$ respectively); and with $m = 5$, $n = 64$ (PPI-[T(C$_5$)]$_{64}$). Only series 1 was investigated because this series provides the first examples of nematic mesomorphism for end-on dendrimers whereas nematic side-on dendrimers have already been described.[4−10] In all cases, the nematic nature was demonstrated by the presence in the X-ray patterns of diffuse scattering alone. The absence of sharp maxima is due to the lack of long-range positional order, whereas the diffuse scattering is related to short-range correlations. The most intense scattering takes place in the wide-angle region, and it corresponds to a distance of about 4.5 Å. This feature results from the average lateral distance between the conformationally disordered dendrimer branches, between the hydrocarbon chains and between the closed-packed mesogenic units. It is commonly observed for the nematic phases formed by monomeric systems. Figure 2 shows a schematic representation of the dendritic structure in the nematic phase for end-on dendrimers.

Determination of the Symmetry for the Nematic Phase of a Side-on Dendrimer. Certain liquid crystal polymers in which the mesogenic groups are attached side-on to the polymer backbone via a flexible spacer are thought to form biaxial nematic phases.[19,20] Indeed this identification, for a naphthalene based mesogenic group, is supported by recent deuterium NMR studies.[21] In addition, at the other extreme of molecular mass a rod-disk liquid crystal dimer, with the rod also attached side-on to the disk, has been found to be highly biaxial and to form a nematic phase with properties suggestive of incipient biaxiality.[22] It seems reasonable, therefore, to expect that the nematic phase formed by the side-on dendrimers might also be biaxial. To investigate this exciting possibility we have determined the symmetry of the nematic phase for PPI-[L(C$_4$)]$_{16}$ using deuterium NMR spectroscopy. In such experiments the objective is to measure the spectrum when one director, e.g., **n**, is aligned parallel to the magnetic field of the spectrom-

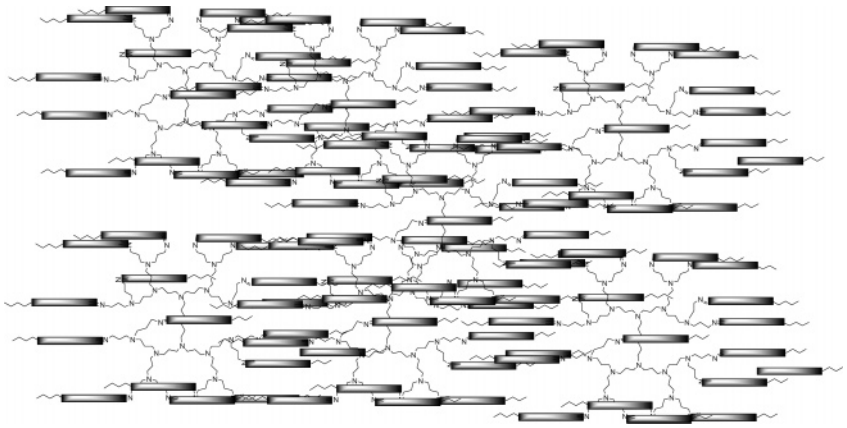

Figure 2. Schematic representation of the dendritic structure in the nematic phase for end-on dendrimers.

eter and then again when it is orthogonal to the field. For a monodomain sample the spectrum for a group of equivalent deuterons is a simple quadrupolar doublet, provided any dipolar couplings are not resolved. For a uniaxial nematic the initial quadrupolar splitting, $\Delta\nu_0$, will be reduced by a factor of 2 when the sample is rotated by 90° and the director, **n**, is aligned orthogonal to the field. The spectral behavior for a biaxial nematic following rotation is, as might be anticipated, somewhat more complex.[23] Initially the remaining two directors, e.g., **l** and **m**, are randomly distributed in the plane orthogonal to **n** and so to the field. After rotation through 90°, the field will be in the plane containing the **l** and **m** directors, and so they will adopt all orientations with respect to this. The observed spectrum is then the sum of spectra from all orientations of the two directors with respect to the field. Accordingly, it will be dominated by the quadrupolar doublets associated with **l** and **m** parallel to the field which correspond to the extreme values of the splittings. Armed with these splittings, it is possible to determine the biaxiality in the partially averaged quadrupolar tensor[24] which is related to, among other things, the phase biaxiality. However, the field will attempt to align the directors in order to minimize the magnetic energy and so the spectrum is expected to change with time. The rate at which the director alignment takes place in comparison with the rate at which the sample can be rotated determines the information content of the spectrum measured immediately following rotation. Techniques have been developed to overcome the problem of field-induced alignment of the directors,[21,25] but as we shall see, we did not need to resort to them here.

In the absence of specifically deuterated dendrimers deuterium was added to the sample in the form of perdeuterated *p*-xylene-d_{10}. This was chosen as the probe because it is found to be sensitive to the phase biaxiality, at least of a crystal E phase, and will not evaporate from the nematic phase.[26] The concentration of the probe was 2.5 wt % in the dendromesogen, PPI-$[L(C_4)]_{16}$, the sample was heated in the NMR tube into the isotropic phase and was mixed mechanically. The deuterium NMR spectra were measured using a Varian Infinity Plus 300 spectrometer at a frequency of 46.04 MHz, corresponding to a field strength of 7.05 T. The choice of sample temperature was a compromise between that deep in the nematic where the phase biaxiality should be large and near the nematic−isotropic transition where the spectral resolution should be high. In our experiments it proved possible to obtain sufficiently well-resolved spectra at temperatures as low as 50 °C. This corresponds to a shifted temperature, $T_{NI} - T$, of 17 °C since the addition of the *p*-xylene probe lowers the nematic−isotropic transition temperature to 67 °C. We have also investigated the phase symmetry at higher temperatures, namely 52, 60, and 65 °C, and we show the results for 52 °C corresponding to a shifted temperature of 15 °C. Initially the tube was rotated manually using the Varian goniometer probe. The time taken to do this was about 30 s, and during this period the director had started to be aligned by the field so that we were not able to determine the phase symmetry from the spectrum obtained after rotation. To overcome this problem, we have used a jump-rotation probe specially developed by Varian in collaboration with Southampton for such experiments. This allows the sample to be turned through 90° in just 20 ms, which proves to be sufficiently short that the field does not align the director during the rotation of the sample. The power spectra obtained prior to rotation and immediately after the jump-rotation are shown in Figure 3. Prior to sample rotation the director, **n**, corresponding to the least negative diamagnetic susceptibility, had been aligned parallel to the magnetic field. The spectrum of this sample consists of two quadrupolar doublets; that with the larger splitting originates from the methyl deuterons while the inner doublet comes from the aromatic deuterons.[27] The intensities of the two doublets are not in the expected ratio of 6:4 because the recycle delay following the quadrupolar echo sequence used to measure the free induction decay (FID) was set at less than its optimum value in order to minimize the time taken to obtain the spectrum. The time taken to record the spectrum was 14 s which is small in comparison with the time taken for the initial alignment of the director following rotation of the sample by 90°. The spectral resolution is not as high as for a low molar mass nematogen[28] which is to be expected given the higher viscosity of the dendromesogen; none the less, the two quadrupolar splittings can be measured with reasonable accuracy. To achieve this we have used a software package to fit individual Lorentzian lines to the four peaks in the spectrum. In this fitting procedure the line position, the line width and the intensity are optimized; the best fit is shown as the solid, noiseless line in Figure 3 and is in good agreement with the experimental spectra. The spectrum when **n** is orthogonal to the field, which is measured immediately following rotation of the sample, retains the two quadrupolar doublets as in the original spectra but with significantly smaller splittings. The fact that there are two and not four splittings could indicate that the phase is uniaxial or, if it is biaxial, that one of the other directors, **l** or **m**, had been aligned by the magnetic field thus producing a uniformly aligned biaxial nematic. Indeed this field-induced alignment has been proposed for the side-on liquid crystal polymer.[21] However, for the dendromesogen, PPI-$[L(C_4)]_{16}$, the quadrupolar splittings obtained by fitting the spectrum, following rotation by 90°, are close to half of their original values. Although the values of the ratio, $|\Delta\nu_{\mathbf{l}}/\Delta\nu_{\mathbf{n}}|$, are close to half, in fact 0.497 for the methyl deuterons and 0.472 for the aromatic deuterons, the small deviation from 0.500 implies that the biaxiality in the quadrupolar tensor is not quite zero. This biaxiality is related to the splittings by[28]

$$\eta = -2|\Delta\nu_{\mathbf{l}}/\Delta\nu_{\mathbf{n}}| + 1$$

where the minus sign originates from the fact that the quadrupolar splittings have opposite signs. This gives η for the methyl deuterons as 0.005 and for the aliphatic deuterons as 0.057. Strictly the biaxialities for the two types of deuteron, methyl and aromatic, are not necessarily the same given their different locations in the *p*-xylene probe; the fact that they are so close to zero allows us to average them to obtain an overall estimate of the biaxiality as 0.031 ± 0.026. We have obtained comparable results for the biaxiality at the other temperatures for which the phase symmetry was determined. To put this result in perspective, we note that the comparable results obtained for D_2O in a lyotropic biaxial nematic phases have been reported[23] as high as 0.7 and 1.0, the latter being the maximum value for η. This comparison strongly suggests that the nematic phase of the dendromesogen, PPI-$[L(C_4)]_{16}$, has uniaxial

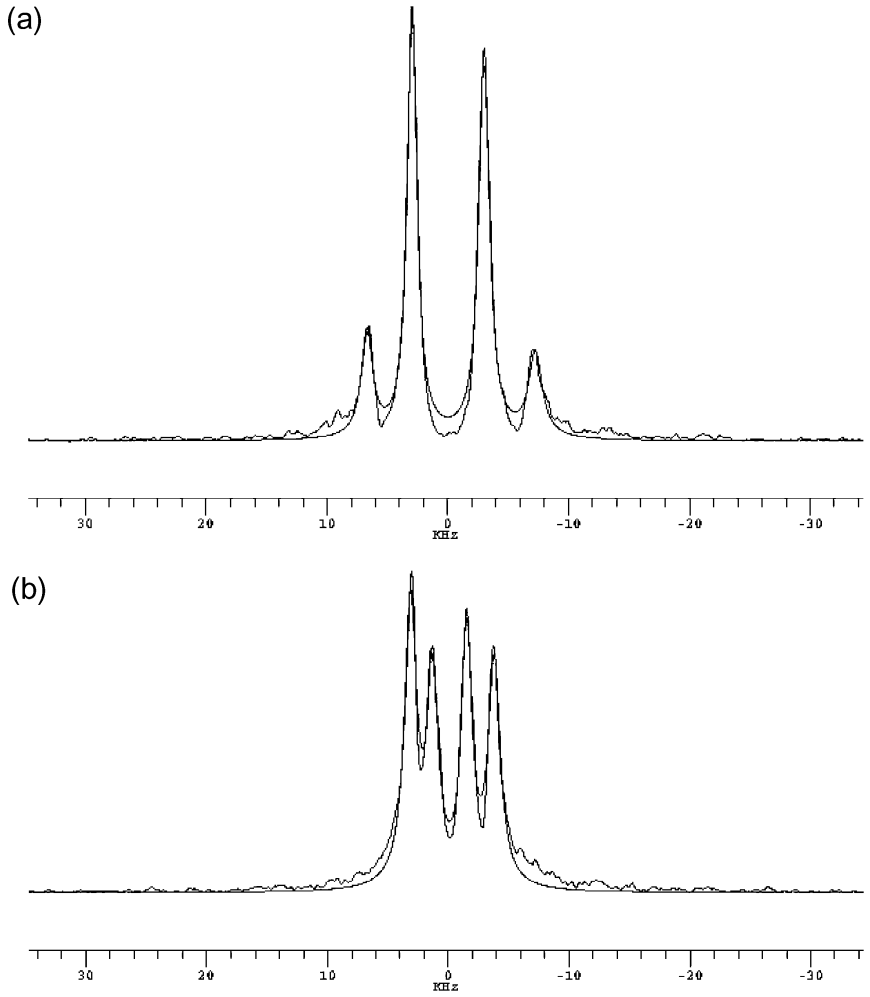

Figure 3. Deuterium NMR spectra of *p*-xylene-d_{10} dissolved in the nematic phase of the dendromesogen, PPI-$[L(C_4)]_{16}$, at 52 °C with (a) the director, **n**, parallel to the magnetic field and (b) immediately after the sample had been rotated by 90°. The solid, noiseless lines shows the best fits to the experimental spectra.

symmetry at least for temperatures as low as 17 °C below the nematic−isotropic transition.

We have achieved our aim of determining the symmetry of the nematic phase. However, the spectra also contain other useful information about the dendromesogen and we shall now discuss this, albeit briefly. First, we note that the quadrupolar splittings are related to the orientational order of the probe in the nematic phase. The values found at 52 °C, which corresponds to a shifted temperature, $T_{NI} - T$, of 15 °C, are 13.93 and 5.96 kHz, for the methyl and aromatic deuterons, respectively. These splittings can be converted into the principal components of the Saupe ordering matrix, **S**, for *p*-xylene.[27] The symmetry and shape of a *p*-xylene molecule require that the *p*-axis is the major axis, *z*, and that the minor axes, *x* and *y*, are in the molecular plane and orthogonal to it, respectively. The major order parameter, S_{zz}, is found to be 0.155 and the biaxiality, $(S_{xx} - S_{yy})$, in the ordering matrix for *p*-xylene in the uniaxial nematic phase is 0.106. These values are somewhat smaller than those determined for the series of 4-alkyloxy-4′-cyanobiphenyls;[27] at the same shifted temperature S_{zz} is about 0.22 and $(S_{xx} - S_{yy})$ is 0.17; however, the precise values do depend slightly on the chain length. Although we are measuring the ordering of a probe molecule, it is expected to reflect the orientational order of the nematic host, and so our results suggest that the order of the dendromesogen is somewhat less than that of low molar mass cyanobiphenyls, as we had found for a codendromesogen with the mesogenic groups attached side-on and end-on.[10] This reduction of the order is consistent with the results for the transitional entropy per mesogenic group, and both are to be anticipated given the smaller volume fraction of mesogenic groups in the dendromesogen.

The other aspect of liquid crystal behavior that our results provide concerns the dynamics of the field-induced alignment of the director. According to theory[29] the angle, $\theta(t)$, made by the director with the aligning magnetic field should vary with time, *t*, according to

$$\tan \theta(t) = \tan \theta_0 \exp(-t/\tau) \quad (1)$$

where the field-induced relaxation time, τ, is

$$\tau = \mu_0 \gamma_1 / \Delta\chi B^2 \quad (2)$$

Provided the nematic is aligned by the field as a monodomain, then we expect to see the quadrupolar splittings increase following rotation of the sample as the angle made by the director with the magnetic field decreases according to eq 1. This follows because the quadrupolar splitting is related to the director orientation by

$$\Delta\upsilon(\theta(t)) = \Delta\upsilon_0 P_2(\cos \theta(t)) \quad (3)$$

where $P_2(\cos \theta(t))$ is the second Legendre function.[30] The

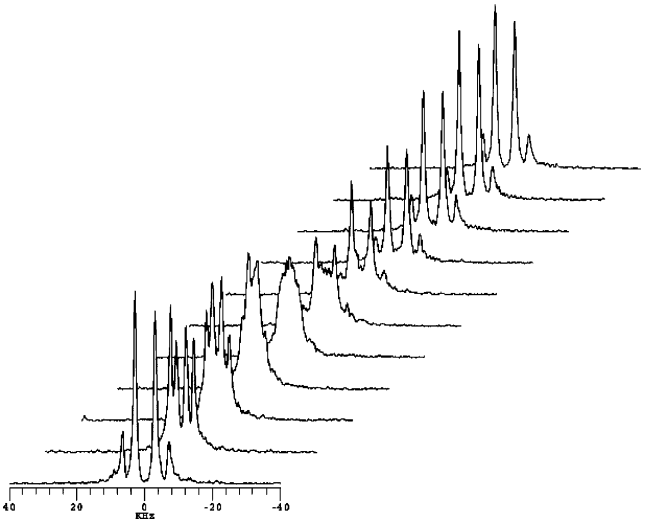

Figure 4. Deuterium NMR spectra of *p*-xylene-d_{10} dissolved in the nematic phase of the dendromesogen, PPI-$[L(C_4)]_{16}$, at 52 °C, before and after the jump-rotation of the sample through 90°. The spectra are separated in time by approximately 14 s.

NMR spectra recorded for *p*-xylene-d_{10} dissolved in the dendromesogen, PPI-$[L(C_4)]_{16}$, are shown as a function of time in Figure 4 where the spectra are separated in time by approximately 14 s, the time also taken to measure each spectrum. Following rotation of the sample, the quadrupolar splittings remain essentially constant suggestive of an induction period during which the director orientation is essentially unchanged. This behavior is in accord with theory, for when the director is almost orthogonal to the field the magnetic torque is very small and so the intial rate at which the director orientation changes is also small.[31] However, the spectral lines do broaden slightly showing that the director distribution is also broadening, as a result of field-induced rearrangement of the director. When the third spectrum is reached, after 42 s, the quadrupolar splittings have changed significantly and the lines have also broadened so that the spectrum is rather featureless. Immediately following this two strong lines appear in the center of the spectrum with a splitting of about 5.8 kHz which is essentially equal to the quadrupolar splitting for the aromatic deuterons when the director is parallel to the magnetic field. This suggests that a significant fraction of the sample now has the director aligned parallel to the field. This conclusion is supported by the presence of two weak lines at the extremities of the spectrum with a splitting of approximately 13.8 kHz corresponding to that of the methyl deuterons prior to sample rotation. With further increase in time, the spectral lines sharpen, but the splittings remain essentially unchanged; indeed, the final three spectra shown in Figure 4 are comparable to the first spectrum recorded before the sample was rotated, showing that the director is now aligned parallel to the magnetic field. It would appear, therefore, that after the director has been rotated to be perpendicular to the magnetic field there is a small broadening of the director distribution during the first 28 s. In contrast, there is a significant change in the director distribution during the next 28 s when the director is essentially aligned parallel to the field. This alignment process appears to be complete after a further 42 s. Our observation that the alignment process is complicated and that the director is not aligned as a monodomain is, perhaps, to be expected because there are clearly two alignment pathways that the director can follow when it is initially orthogonal to the field. This degeneracy in alignment results in the creation of inversion walls which separate regions of the nematic where the directors are moving in opposite directions and so the sample is not aligned as a monodomain.[32] In consequence, we cannot use the splittings, together with eqs 1 and 3, to determine the magnetic field-induced relaxation time. However, a crude estimate of this can be obtained from the time taken to align the director following rotation through 90°, which is about 98 s. This time can be compared to that found for the alignment of the director in the low molar mass nematic, 4-pentyl-4′-cyanobiphenyl, which under comparable conditions was found to be about 7 ms.[33] The creation of the dendromesogen has, therefore, resulted in a dramatic increase in the relaxation time and hence the rotational viscosity by a factor of approximately 10^4.

Conclusions

In conclusion, we have created a new class of dendrimers which exhibit nematic phases. These results indicate that the synthesis of these nanophase-structured dendrimers leads to macromolecules with LC properties similar to those of comparable low molar mass compounds. One of the lateral nematic dendrimers PPI-$[LC_4]_{16}$ synthesized exhibits a uniaxial nematic mesophase at least as low as 17 °C below the nematic−isotropic transition contrary to what we had expected based on the behavior described for lateral nematic liquid crystal polymers.[20,21]

Experimental Section

Techniques. Microanalyses were performed with a Perkin-Elmer C H N 2400 microanalyzer in the Servicio Interdepartamental de Investigación (SIDI) of the Universidad Autónoma of Madrid. Infrared spectra were obtained with a Perkin-Elmer 1600 (FTIR) spectrophotometer in the 400−4000 cm^{-1} spectral range. ^1H and ^{13}C NMR spectra were recorded on a Bruker Unity 300 MHz spectrometer. Mass spectra were obtained with a VG Autospec spectrometer with positive-ion FAB (FAB^+) (3-nitro benzyl alcohol (NBA)). MALDI−TOF mass spectrometry was carried out on a REFLEX III instrument (BRUKER) using ditranol as a matrix in the Servicio Interdepartamental de Investigación (SIDI) of the Universidad Autónoma of Madrid. Gel permeation chromatography (GPC) was carried out in a Waters liquid chromatography system equipped with a 600E multisolvent delivery system and 996 photodiode array detector. Two Ultrastyragel columns (Waters, pore sizes 500 and 10^4 Å) were connected in series. The CH_2Cl_2 was used as the mobile phase with a flow rate of 0.8 $mLmin^{-1}$. Calibration was performed with polystyrene standards. The optical textures of the mesophases were studied with a Olympus polarizing microscope equipped with a Linkam THMS 600 hot-stage and an Linkam TMS 91 central processor. The transition temperatures and enthalpies were measured by differential scanning calorimetry with a Perkin-Elmer DSC-7 instrument operated at a scanning rate of 10 °C min^{-1} on heating and cooling. The apparatus was calibrated with indium (156.6 °C; 28.4 J g^{-1}) as the standard. The XRD patterns were obtained with a pinhole camera (Anton-Paar) operating with a point-focused Ni-filtered Cu Kα beam. The sample was held in Lindemann glass capillaries (1 mm diameter). The capillary axis is perpendicular to the X-ray beam and the pattern is collected on flat photographic film perpendicular to the X-ray beam. Spacing were obtained via Bragg's law.

Chemicals. 4-Substituted-benzoic acids, *N,N′*-dicyclohexylcarbodiimide (DCC), 4-(dimethylamino)pyridine (DMAP), and poly(propyleneimine) (PPI) ($G = 1, 2, 3, 4, 5$) were purchased

from the Aldrich Chemical Co. All of these substances were used without further purification. Dry dichloromethane (refluxed over calcium chloride, distilled and stored over molecular sieves 4 Å) was used as the reaction solvent. All atmosphere sensitive reactions were carried out under dry argon. Analytical TLC was performed on Kieselgel F-254 precoated silicagel plate (SDS). Visualization of the spots was accomplished with UV light (254 nm).

Synthesis. Series 1. We give here the general procedure for the condensation of 4-(4-alkoxybenzoyloxy)-2-hydroxybenzaldehydes with poly(propylene inine) dendrimers of the first to fifth generation PPI-$(NH_2)_n$, n = 4, 8, 16, 32, and 64. To a stirred solution of the 4-substituted salicylaldehyde (1 mmol) in CH_2Cl_2 (15 mL) was added neutral activated grade I alumina (0.5 g) and then the corresponding PPI_n (1/n mmol). The mixture was refluxed under argon for 12 h. The alumina was filtered off and the solvent from the filtrate evaporated under vacuum. The resulting solid was purified by column chromatography using CH_2Cl_2 as eluent or by dissolving in CH_2Cl_2 and precipitating the dendrimer with methanol and then centrifugation; this procces was repeated several times until pure by NMR. Absence of primary amine groups was checked by the ninhydrine test. (Yield: 55−75%.)

Series 2. General Procedure for the Preparation of the Side-on Liquid Crystalline Dendrimers. Compound **14** (186 mg, 0.225 mmol) was dissolved in dry dichloromethane (20 mL) under an argon atmosphere. A poly(propyleneimine) dendrimer of the appropriate generation (90 mg, 0.026 mmol) was dissolved in dry dichloromethane (10 mL) and added to the stirred solution of the promesogenic units. On mixing, the initially transparent solutions became turbid. The mixture was stirred under reflux for 7 days, diluted with dichloromethane (50 mL), and washed with NaOH solution (2%) (2 × 20 mL). The combined aqueous phases were again extracted with dichloromethane and the combined organic phases were dried over anhydrous sodium sulfate and concentrated in vacuo. The crude product was purified by column chromatography using dichloromethane/hexane (1/2) as eluent. If any impurity were detected by GPC, the product was dissolved in the minimum volume of dichloromethane and precipitated with hexane or ethanol. Absence of primary amine groups was checked by the ninhydrine test. Yield: 30−50%.

Characterization. The purity of each compound (intermediate and dendrimers) was confirmed by elemental analysis, ^{1}H NMR, ^{13}C NMR, IR spectroscopy, FAB$^+$ or MALDI−TOF MS, and GPC. Because of the similarity of IR, ^{1}H NMR, and ^{13}C NMR spectra of these materials, we only quote data for PPI-$[T(C_2)]_{16}$ and PPI-$[L(C_4)]_{16}$ dendrimers as representative examples. Data obtained from other techniques are gathered in Tables 1 and 2.

PPI-$[T(C_2)]_{64}$. IR (Nujol, cm^{-1}): $\tilde{\nu}$ = 3435.0 (O−H), 1731.2 (OC=O), 1631.8 (C=N). ^{1}H NMR ($CDCl_3$, 400 MHz): δ = 1.25 (s broad, 4H, $-NCH_2CH_2CH_2CH_2N-$) 1.39 (s broad, 192H, $-CH_2CH_3$,), 1.48−1.82 (m, 248H, $CH_2CH_2CH_2N=$, $-CH_2(CH_2N)_2$), 2.43 (s broad, 372H, $NCH_2CH_2CH_2N-$, $-NCH_2CH_2CH_2CH_2CH_2N-$) 3.48 (s broad, 128H, $CH_2CH_2N=CH-$), 3.95−4.08 (m, 128H, $-CH_2CH_3$,), 6.56 (d, J = 7.6 Hz, 64H, ArH), 6.69 (s broad, 64H, ArH), 6.85−6.92 (m, 128H, ArH), 7.09 (d, J = 7.6 Hz, 64H, ArH), 7.97−8.10 (m, 128H, ArH), 8.15 (s broad, 64H, $-N=CH-$), 13.96 (s broad, 64H $-OH$). ^{13}C NMR APT ($CDCl_3$, 100 MHz): δ = 14.6 ($-CH_2CH_3$), 24.3, 24.2 ($CH_2CH_2N=$, $-CH_2(CH_2N)_2$), 28.4 ($CH_2CH_2CH_2N=$), 51.3, 52.0, 52.1 ($-CH_2N-$), 56.6 ($CH_2N=CH-$), 63.6 ($-OCH_2-$), 110.4, 112.0, 114.1, 116.4, 121.4, 132.1, 132.2, (ArC), 154.0, 163.2, 163.4, (C quarter), 164.1 ($CH=N$), 164.3 (C quarter).

PPI-$[L(C_4)]_{16}$. IR (Nujol, cm^{-1}): $\tilde{\nu}$ = 3294 (CON−H), 1728 (OC=O), 1640 (OC−NH); ^{1}H NMR ($CDCl_3$, 400 MHz): δ = 0.96 (m, $-(CH_2)_2CH_3$), 1.05−1.30 (m, $-ArCOOCH_2CH_2(CH_2)_6CH_2CH_2CONH-$, $-NCH_2CH_2CH_2CH_2N-$), 1.35−1.60 (m, $ArCOOCH_2(CH_2)_7CH_2CH_2CONH-$, $ArOCH_2CH_2CH_2CH_3$, $-NCH_2CH_2CH_2N-$), 1.65−1.90 (m, $-NCH_2CH_2CH_2NH(O)C-$, $ArOCH_2CH_2CH_2CH_3$, $ArCOOCH_2CH_2(CH_2)_7CH_2CONH-$), 2.12 (t, J = 7.6 Hz $-NH(O)CCH_2CH_2-$), 2.35 (bs, $-NCH_2CH_2CH_2CH_2N-$, $-NCH_2CH_2CH_2CH_2N-$, $-NCH_2CH_2CH_2NH(O)C-$), 3.21 (bs, $-NCH_2CH_2CH_2NH(O)C-$), 4.02 (m, $ArOCH_2(CH_2)_3CH_3$), 4.10 (t, J = 6.8 Hz, $ArCOOCH_2CH_2-$), 6.95 (m, ArH), 7.05 (bs, C(O)NH), 7.23 (d, J = 8.6 Hz, ArH), 7.42 (dd, J_1 = 2.8 Hz, J_2 = 8.6 Hz, ArH), 7.86 (d, J = 2.8 Hz, ArH), 8.12 (m, ArH). ^{13}C NMR ($CDCl_3$ 100 MHz): δ = 13.81, 19.16, 24.37, 25.79, 25.91, 27.02, 28.36, 29.19, 29.43, 29.65, 31.08, 36.55, 37.68, 51.33, 52.05, 65.57, 67.96, 68.00, 114.29, 114.36, 120.91, 121.35, 124.90, 124.98, 127.05, 132.32, 132.39, 148.05, 148.28, 163.57, 163.73, 164.06, 164.51, 164.87.

Acknowledgment. This work has been supported by the CICYT of Spain (MAT 2002-04118-C02-01 and MAT 2003-07806-C01) and FEDER (EU). The European Union (HPRN−CT2000-00016), and Diputación General de Aragón (DGA) (Spain). R.M.-R. acknowledges a fellowship from MEC (Spain). M.McK. acknowledges a fellowship from EU and L.P acknowledges a collaboration fellowship from MEC (Spain). G.R.L. thanks the Higher Education Funding Council for England for a grant (JR00SOLEEQ) under the 2000 JREI to cover the cost of the Varian spectrometer. We are also grateful to Mr. O. G. Johannessen (Southampton) for commissioning the jump rotation probe. A.M. acknowledges the Government of Malaysia and the Universiti Malaya for the award of a Scholarship.

References and Notes

(1) Fréchet J. M., and Tomalia D. A. *Dendrimers and Other Dendritic Polymers*; Wiley Series on Polymer Science; John Wiley and Sons, Ltd.: New York, 1999.
(2) Newkome, G. R.; Moorefield, C. N.; Vögtle, F. *Dendrimers and Dendrons: Concepts, Synthesis, Applications*; Wiley-VCH Verlag GmbH: Weinheim, Germany, 2001.
(3) Marcos, M.; Omenat, A.; Serrano, J. L. *C. R. Chim.* **2003**, *6*, 947−957.
(4) Barberá, J.; Giménez, R.; Marcos, M.; Serrano, J. L. *Liq. Cryst.* **2002**, *29*, 309−314.
(5) Elsässer, R.; Mehl, G. H.; Goodby, J. W.; Veith, M. *Angew. Chem., Int. Ed.* **2001**, *40*, 2688−2690.
(6) Saez, I. M.; Goodby, J. W.; Richardson, R. M. *Chem.—Eur. J.* **2001**, *7*, 2758−2764.
(7) Saez, I. M.; Goodby, J. W. *J. Mater. Chem.* **2001**, *11*, 2845−2851.
(8) Saez, I. M.; Goodby, J. W. *J. Mater. Chem.* **2003**, *13*, 2727−2739.
(9) Saez, I. M.; Goodby, J. W. *Chem.—Eur. J.* **2003**, *9*, 4869−4877.
(10) Martín-Rapún, R.; Marcos, M.; Omenat, A.; Serrano, J. L.; Luckhurst, G.; Mainal, A. *Chem. Mater.,* in press.
(11) Barberá, J.; Marcos, M.; Serrano, J. L. *Chem.—Eur. J.* **1999**, *5*, 1834−1840.
(12) Hessel, F.; Finkelmann, H. *Polym. Bull. (Berlin)* **1985**, *14*, 375−378.
(13) Keller, P.; Harduin, F.; Mauzac, M.; Achard, M. F. *Mol. Cryst. Liq. Cryst.* **1988**, *155*, 171−178.
(14) Hassner, A.; Alexanian, V. *Tetrahedon Lett.* **1978**, 4475−4478.
(15) Keller, P.; Thomsen, D. L., III; Li, M.-H. *Macromolecules* **2002**, *35*, 581−584.
(16) Baars, M. W. P. I.; Söntjens, S. H. M.; Fischer, H. M.; Peerlings, H. W. I.; Meijer, E. W. *Chem.—Eur. J.* **1998**, *4*, 2456−2466.
(17) Dubin, P. L.; Edwards, S. L.; Kaplan, J. L.; Mehta, M. S.; Tomalia, D. T.; Xia, J. *Anal. Chem.* **1992**, *64*, 2344−2347.
(18) Demus, D.; Richter, L. *Textures of Liquid Crystals;* V. E. B. Deutscher Verlag für Gründstoffindustrie: Leipzig, Germany, 1978.
(19) Hessel, F.; Herr, R. P.; Finkelmann, H. *Makromol. Chem.* **1987**, *188*, 1597−1611.
(20) Leube, H. F.; Finkelmann, H. *Makromol. Chem.* **1991**, *192*, 1317−1328.
(21) Severing, K.; Saalwachter, K. *Phys. Rev. Lett.* **2004**, *92*, 125501−1−4.
(22) Hunt, J. J.; Date, R. W.; Timimi, B. A.; Luckhurst, G. R.; Bruce, D. W. *J. Am. Chem. Soc.* **2001**, *123*, 10115−6.
(23) Nicoletta, F. P.; Chidichimo, G.; Golemme, A.; Picci, N. *Liq. Cryst.* **1991**, *10*, 665−674.

(24) Fan, S. M.; Fletcher, I. D.; Gündogan, B.; Heaton, N. J.; Kothe, G.; Luckhurst, G. R.; Praefcke, K. *Chem. Phys. Lett.* **1993**, *204*, 517−523.
(25) Yu, L. J.; Saupe, A. *Phys. Rev. Lett.* **1980**, *45*, 1000−1003.
(26) Dabrowski, R.; Luckhurst, G. R.; Mainal, A. Presented at the 20th International Liquid Crystal Conference, Ljubljana, Slovenia, 2004; Poster STR-P097.
(27) Emsley, J. W.; Luckhurst, G. R.; Sachdev, H. S. *Liq. Cryst.* **1989**, 5, 953−967.
(28) Luckhurst, G. R. *Thin Solid Films* **2001**, *393*, 40−52.
(29) Wise, R. A.; Olah, A.; Doane, J. W. *J. Phys. (Paris)* **1975**, *36* (C1), 117−120.
(30) Luckhurst, G. R.; Miyamoto, T.; Sugimura, A.; Timimi, B. A. *J. Chem. Phys.* **2002**, *116*, 5099−5106.
(31) Bras, W.; Emsley, J. W.; Levine, Y. K.; Luckhurst, G. R.; Seddon, J. M.; Timimi, B. A. *J. Chem. Phys.* **2004**, *121*, 4397−4413.
(32) Esnault, P.; Casquilho, J. P.; Volino, F.; Martins, A. F.; Blumstein, A. *Liq. Cryst.* **1990**, *7*, 607−628.
(33) Luckhurst, G. R.; Miyamoto, T.; Sugimura, A.; Timimi, B. A. *Thin Solid Films* **2001**, *393*, 399−406.

MA048450P